Prepared for submission to JCAP

IFIC/10-38

Constraining the cosmic radiation density due to lepton number with Big Bang Nucleosynthesis

Gianpiero Mangano,[a] **Gennaro Miele,**[a,b] **Sergio Pastor,**[c] **Ofelia Pisanti,**[a,b] **and Srdjan Sarikas**[a,b]

[a]Istituto Nazionale di Fisica Nucleare - Sezione di Napoli
Complesso Universitario di Monte S. Angelo, I-80126 Napoli, Italy
[b]Dipartimento di Scienze Fisiche, Università di Napoli *Federico II*
Complesso Universitario di Monte S. Angelo, I-80126 Napoli, Italy
[c]Instituto de Física Corpuscular (CSIC-Universitat de València),
Ed. Institutos de Investigación, Apdo. correos 22085, E-46071 Valencia, Spain
E-mail: mangano@na.infn.it, miele@na.infn.it, pastor@ific.uv.es,
pisanti@na.infn.it, sarikas@na.infn.it

Abstract. The cosmic energy density in the form of radiation before and during Big Bang Nucleosynthesis (BBN) is typically parameterized in terms of the effective number of neutrinos $N_{\rm eff}$. This quantity, in case of no extra degrees of freedom, depends upon the chemical potential and the temperature characterizing the three active neutrino distributions, as well as by their possible non-thermal features. In the present analysis we determine the upper bounds that BBN places on $N_{\rm eff}$ from primordial neutrino–antineutrino asymmetries, with a careful treatment of the dynamics of neutrino oscillations. We consider quite a wide range for the total lepton number in the neutrino sector, $\eta_\nu = \eta_{\nu_e} + \eta_{\nu_\mu} + \eta_{\nu_\tau}$ and the initial electron neutrino asymmetry $\eta^{\rm in}_{\nu_e}$, solving the corresponding kinetic equations which rule the dynamics of neutrino (antineutrino) distributions in phase space due to collisions, pair processes and flavor oscillations. New bounds on both the total lepton number in the neutrino sector and the $\nu_e - \bar{\nu}_e$ asymmetry at the onset of BBN are obtained fully exploiting the time evolution of neutrino distributions, as well as the most recent determinations of primordial ^{2}H/H density ratio and ^{4}He mass fraction. Note that taking the baryon fraction as measured by WMAP, the ^{2}H/H abundance plays a relevant role in constraining the allowed regions in the $\eta_\nu - \eta^{\rm in}_{\nu_e}$ plane. These bounds fix the maximum contribution of neutrinos with primordial asymmetries to $N_{\rm eff}$ as a function of the mixing parameter θ_{13}, and point out the upper bound $N_{\rm eff} \lesssim 3.4$. Comparing these results with the forthcoming measurement of $N_{\rm eff}$ by the Planck satellite will likely provide insight on the nature of the radiation content of the universe.

Keywords: Neutrinos, physics of the early universe, primordial asymmetries

ArXiv ePrint: 1011.0916

1 Introduction

The dynamics of neutrino oscillations in the early universe has been extensively studied in the scientific literature and is expected to have produced an efficient mixing of flavor neutrino distributions at a temperature $T_\gamma \sim 1$ MeV, thus shortly before the freezing of the neutron-to-proton density ratio and the onset of Big Bang Nucleosynthesis (BBN). Indeed, while flavor neutrino conversions are suppressed by matter effects at larger temperatures, at $T_\gamma \sim 10$ MeV the atmospheric mass-squared difference $\Delta m^2_{\rm atm}$ triggers efficient $\nu_\mu - \nu_\tau$ mixing, as well as $\nu_x - \nu_e$ ($x = \mu, \tau$) conversions if the angle θ_{13} is not vanishing and sufficiently large. Finally, at $T_\gamma \lesssim 3$ MeV oscillations driven by $\Delta m^2_{\rm sol}$ set on and are large enough to achieve strong flavor conversions before BBN [1–4].

These results have a major impact on the possible values for the cosmological lepton asymmetry stored in each neutrino flavor, which in analogy with the baryon-antibaryon asymmetry parameter $\eta_b = (n_b - n_{\bar b})/n_\gamma$, can be parameterized by the number density ratios

$$\eta_{\nu_\alpha} = \frac{n_{\nu_\alpha} - n_{\bar\nu_\alpha}}{n_\gamma} \quad , \quad \alpha = e, \mu, \tau \quad . \tag{1.1}$$

Based on the equilibration of lepton and baryon asymmetries by sphalerons in the very early universe, such a neutrino asymmetry should be of the same order of the cosmological baryon number $\eta_b = 273.93\,\Omega_b h^2\,10^{-10}$, which is restricted to be a few times 10^{-10} by present observations, such as 7-year data from the WMAP satellite and other cosmological measurements [5]. Nevertheless, a cosmological neutrino asymmetry orders of magnitude larger than this value is still an open possibility, with implications on fundamental physics in the early universe, such as their potential relation with the cosmological magnetic fields at large scales [6]. In particular, a non-zero lepton asymmetry leads to an enhanced contribution of neutrinos to the energy density in the form of radiation ρ_r, which, after the e^+e^- annihilation phase, is usually parameterized as $\rho_r/\rho_\gamma = 1 + 7/8(4/11)^{4/3} N_{\rm eff}$. The parameter $N_{\rm eff}$ is the "effective number of neutrinos" whose standard value is 3 in the limit of instantaneous neutrino decoupling. Interestingly, recent data on the anisotropies of the cosmic microwave background from WMAP [5] and the primordial ^{4}He abundance [7–9] seem to favor a value of $N_{\rm eff} > 3$, although with large errorbars.

If neutrinos are in kinetic and chemical equilibrium, their distribution of momenta is parameterized by a temperature and a well defined chemical potential μ_{ν_α}, and each flavor neutrino asymmetry can be expressed in terms of the corresponding degeneracy parameter $\xi_{\nu_\alpha} \equiv \mu_{\nu_\alpha}/T_{\nu_\alpha}$ as

$$\eta_{\nu_\alpha} = \frac{1}{12\zeta(3)} \left(\frac{T_{\nu_\alpha}}{T_\gamma}\right)^3 \left(\pi^2 \xi_{\nu_\alpha} + \xi^3_{\nu_\alpha}\right) \quad . \tag{1.2}$$

In this case, if flavor oscillations enforce the condition that all ξ_{ν_α} are almost the same during BBN, the stringent bound on the electron neutrino degeneracy, which directly enters the neutron/proton chemical equilibrium [10], applies to all flavors. The common value of the neutrino degeneracies is restricted to the range $-0.021 \leq \xi_{\nu_\alpha} \leq 0.005$, $\alpha = e, \mu, \tau$ [11] (see also [12–19] for other analyses). This in turn also implies that, *if neutrinos indeed, reach perfect kinetic and chemical equilibrium before they decouple*, any large excess in cosmic radiation density, if observed, must be ascribed to extra relativistic degrees of freedom since the additional contribution to radiation density due to non vanishing ξ_{ν_α} is very small. Assuming that the neutrino distributions are given by their equilibrium form, the BBN bound

on the neutrino degeneracies leads to the following upper limit on the excess contribution to $N_{\rm eff}$ [2],

$$\Delta N_{\rm eff} = \sum_{\alpha=e,\mu,\tau} \left[\frac{30}{7} \left(\frac{\xi_{\nu_\alpha}}{\pi} \right)^2 + \frac{15}{7} \left(\frac{\xi_{\nu_\alpha}}{\pi} \right)^4 \right] \lesssim 0.0006 \ , \tag{1.3}$$

which is tiny, even compared with the value of $N_{\rm eff} = 3.046$ found solving the neutrino kinetic equations in absence of asymmetries [20].

Neutrino kinetic and chemical equilibrium is maintained in the early universe by purely leptonic weak processes such as neutrino-neutrino interactions, ν-$e^\pm$ scatterings and pair processes, $\nu\bar{\nu} \leftrightarrow e^+e^-$, whose rates become of the order of the Hubble parameter at $T_\gamma \sim 2-3$ MeV. Baryons play no role in this concern due to their very low density. At lower temperatures weak interactions are no longer effective, neutrinos decouple from the rest of the primeval plasma and their distribution in phase space is frozen out. Flavor oscillations driven by $\Delta m^2_{\rm atm}$ take place when neutrinos are still fastly scattering off the surrounding medium, so that the changes in their distribution due to oscillations are efficiently readjusted into an equilibrium Fermi-Dirac function. Instead, flavor conversions due to $\Delta m^2_{\rm sol}$ and θ_{12} occur around neutrino decoupling. This implies, at least in principle, that if neutrinos succeed in achieving comparable asymmetries in all flavors before BBN, their distributions might acquire distortions with respect to equilibrium values due to inefficient interactions.

This can be easily understood by a simple example. Suppose that at temperatures higher than $2-3$ MeV we start with a vanishing total asymmetry, but $\eta^{\rm in}_{\nu_e} = -2\eta^{\rm in}_{\nu_x} \neq 0$ and we artificially switch-off scattering and pair processes. Due to solar-scale oscillations, in the case of maximal mixing asymmetries in each flavor will eventually vanish, but the neutrino distributions will not correspond to equilibrium, since averaging two equilibrium distributions with a different chemical potential does not correspond to a Fermi-Dirac function. Only scatterings and pair-processes can turn it into an equilibrium distribution with, in this case, zero chemical potential.

Though this example is quite extreme and unrealistic, nevertheless, it tells us that the interplay of neutrino freeze–out and $\Delta m^2_{\rm sol}$ oscillation phases might deserve a more careful scrutiny, as first discussed in [21]. In fact, depending on the initial flavor neutrino asymmetries and the value of θ_{13}, the final neutrino distributions at the onset of BBN might show non-thermal distortions which change the neutron-proton chemical equilibrium due to the direct role played by electron (anti)neutrinos. Moreover, this corresponds to an asymmetry-depending parameter $N_{\rm eff} > 3$ which is due to inefficient entropy transfer to the electromagnetic plasma and is not given by the equilibrium value of eq. (1.3). As pointed out in [21] these features will prove to be quite important in case of large initial asymmetries and opposite values for ν_e and $\nu_{\mu,\tau}$ chemical potentials. It was shown that with fine-tuned initial asymmetries the BBN bound could be respected and at the same time an excess radiation density could survive, corresponding to values of $\Delta N_{\rm eff}$ of order unity or larger.

In the present work we extend the analysis of [21] in two ways. First, we consider a wider range of values of the initial neutrino asymmetries and solve their evolution with the corresponding kinetic equations, including both collisions and oscillations. Moreover, the obtained shape of the neutrino distributions is then plugged into the BBN dynamics allowing, by the comparison between the theoretical results and the experimental data on primordial abundances of deuterium and ^{4}He, to find more accurate bounds on the total lepton asymmetry stored in the neutrino sector, as well as the way it was distributed at some early stage in the ν_e and ν_x flavors. In fact, for all initial values of neutrino asymmetries which

are compatible with BBN bounds, the distortions in the neutrino distribution are typically quite small, see Section 2, so that it is accurate enough for our purposes to parameterize them in terms of a Fermi-Dirac function with two time-dependent parameters, which correspond to the first two moments of the actual distribution: an effective chemical potential ξ_{ν_α} and an effective temperature T_{ν_α}, or equivalently, the asymmetry in each flavor and the energy density.

The paper is organized as follows. After setting in Section 2 the formalism of kinetic equations which rule the evolution of neutrino distributions written in the standard density matrix formalism and showing an example of their dynamics, we then study the BBN constraints on neutrino asymmetries in Section 3. In particular, we discuss the experimental data which are used in our analysis for ^{2}H/H and ^{4}He mass fraction Y_p, as well as the way we have modified the public BBN numerical code `PArthENoPE` [22–24] to track neutrino evolution. Finally, we report the bounds on initial (at $T_\gamma \sim 10$ MeV) neutrino asymmetries or their final values after flavor oscillation phase. In Section 4 we give our concluding remarks.

2 The dynamics of neutrinos in the early universe with primordial asymmetries

Our first aim is to calculate the evolution of the three active neutrino distributions in the epoch of the universe right before BBN, when these particles were interacting among themselves and with electrons and positrons. The corresponding weak collision rate decreases very fast with the expansion until neutrinos decouple at $T_\gamma \sim 1$ MeV. At the same time, it was shown in [1–4, 25] that for the neutrino mixing parameters currently allowed, flavor oscillations start to be effective at similar temperatures. In such a case the best way to describe neutrino distributions is to use matrices in flavor space [26, 27]. Since we consider only the three active neutrino species, we will need 3×3 matrices in flavor space $\varrho_{\mathbf{p}}$ for each neutrino momentum $\mathbf{p}$, where the diagonal elements are the usual flavor distribution functions (occupation numbers) and the off-diagonal ones encode phase information and vanish for zero mixing.

Oscillations in flavor space of the three active neutrinos are driven by two mass-squared differences and three mixing angles bounded by the experimental observations in the following ranges: the "solar" $\Delta m^2_{\rm sol} = 7.59^{+0.44}_{-0.37} \times 10^{-5}$ eV^2, the "atmospheric" $|\Delta m^2_{\rm atm}| = 2.40^{+0.24}_{-0.22} \times 10^{-3}$ eV^2 and correspondingly, the large mixing angles $\sin^2\theta_{12} = 0.32^{+0.04}_{-0.03}$ and $\sin^2\theta_{23} = 0.50^{+0.13}_{-0.11}$ (2σ ranges from [28]). On the other hand, the third angle is quite small, $\sin^2\theta_{13} \leq 0.053$ (3σ) [28], even compatible with a vanishing value, though a mild evidence for $\sin^2\theta_{13} > 0$ has been found in global data analyses (see e.g. [29, 30]).

The equations of motion (EOMs) for $\varrho_{\mathbf{p}}$ are the same as those considered in reference [21],

$$\mathrm{i}\,\frac{d\varrho_{\mathbf{p}}}{dt} = [\Omega_{\mathbf{p}}, \varrho_{\mathbf{p}}] + C[\varrho_{\mathbf{p}}, \bar{\varrho}_{\mathbf{p}}]\,, \tag{2.1}$$

and similar for the antineutrino matrices $\bar{\varrho}_{\mathbf{p}}$. The first term on the r.h.s. describes flavor oscillations,

$$\Omega_{\mathbf{p}} = \frac{\mathsf{M}^2}{2p} + \sqrt{2}\,G_{\rm F}\left(-\frac{8p}{3m_{\rm w}^2}\,\mathsf{E} + \varrho - \bar{\varrho}\right)\,, \tag{2.2}$$

where $p = |\mathbf{p}|$ and M is the neutrino mass matrix (opposite sign for antineutrinos). Matter effects are included via the term proportional to the Fermi constant $G_{\rm F}$, where E is the 3×3 flavor matrix of charged-lepton energy densities [26]. For our range of temperatures we only

need to include the contribution of electrons and positrons. Finally, the last term arises from neutrino-neutrino interactions and is proportional to $\varrho - \bar{\varrho}$, where $\varrho = \int \varrho_{\mathbf{p}}\, \mathrm{d}^3\mathbf{p}/(2\pi)^3$ and similar for antineutrinos. For the relevant values of neutrino asymmetries this matter term dominates and leads to synchronized oscillations [2–4]. The last term in eq. (2.1) corresponds to the effect of neutrino collisions, i.e. interactions with exchange of momenta. Here we follow the same considerations of ref. [21], where the reader can find more details on the approximations made and related references. In short, the collision terms for the off-diagonal components of $\varrho_{\mathbf{p}}$ in the weak-interaction basis are momentum-dependent damping factors, while collisions and pair processes for the diagonal $\varrho_{\mathbf{p}}$ elements are implemented without approximations solving numerically the collision integrals as in [20]. These last terms are crucial for modifying the neutrino distributions to achieve equilibrium with $e^{\pm}$ and, indirectly, with photons.

We have solved numerically the EOMs for the matrices in flavor space of neutrinos and antineutrinos with non-zero initial asymmetries. The expansion of the universe is taken into account using comoving variables as in [2], where it was shown that flavor oscillations between muon and tau neutrinos take place at $T_\gamma > 10$ MeV, when interactions are very effective. For any initial values of the muon or tau neutrino asymmetries, the combined effect of oscillations and collisions is able to equilibrate the two flavors and hence leads to $\eta^{\rm in}_{\nu_\mu} = \eta^{\rm in}_{\nu_\tau} \equiv \eta^{\rm in}_{\nu_x}$. Therefore, we start our numerical calculations for each case at $T = 10$ MeV and initial parameters $\eta^{\rm in}_{\nu_e}$ and the total asymmetry $\eta_\nu = \eta^{\rm in}_{\nu_e} + 2\,\eta^{\rm in}_{\nu_x}$. Note that hereafter by η_ν we denote the initial value of the total asymmetry, which is kept constant until the onset of $e^+ - e^-$ annihilations, when it is diluted by the increase of the photon density (as in the case of the baryon asymmetry η_b).

All neutrino mixing parameters, except for θ_{13}, are taken as the best-fit values in [28]. Modifying these parameters within their allowed regions does not affect our results. Instead, the value of θ_{13} plays an important role in the evolution of the neutrino asymmetries [21]. We thus consider either $\theta_{13} = 0$ or $\sin^2\theta_{13} = 0.04$, a value close to the upper bound from neutrino experiments [28–30].

Let us describe the evolution of the flavor asymmetries with a specific example. As shown in [21], large initial values of flavor primordial asymmetries could satisfy the BBN bound only if $\eta^{\rm in}_{\nu_e}$ and $\eta^{\rm in}_{\nu_x}$ have opposite signs and the total asymmetry is not very different from zero. A case with $\eta_\nu = 0$ was the main example presented in [21]. Here we choose instead a benchmark case with non-zero negative total asymmetry, $\eta_\nu = -0.41$, and $\eta^{\rm in}_{\nu_e} = 0.82$. The evolution of the flavor asymmetries is found from the numerical solution of the EOMs and is shown in Figure 1. Other choices of the initial asymmetries will lead to different final values, but the overall behavior of the evolution is similar to the case shown here.

One can see in Figure 1 the effect of flavor oscillations on the evolution of neutrino asymmetries with the universe temperature and the dependence on the value of θ_{13}. If this mixing angle is close to the present experimental upper bound, flavor oscillations are effective around $T_\gamma \sim 8$ MeV (inner red lines) when neutrinos are still in good thermal contact with the ambient plasma.[1] The neutrino distributions evolve keeping an equilibrium form, and the total asymmetry is almost equally distributed among the three flavors. However, the final value of the electron neutrino asymmetry is too different from zero and this case is not allowed by BBN, as we will see in Section 3. Instead, for $\theta_{13} = 0$ flavor oscillations begin only at $T_\gamma \lesssim 3$ MeV, when weak interactions are not frequent enough to keep the neutrino

[1] Here we consider only the case of normal hierarchy, $\Delta m^2_{\rm atm} > 0$. If we choose an inverted hierarchy the results are very similar, except that equilibrium among the flavor asymmetries is reached slightly earlier.

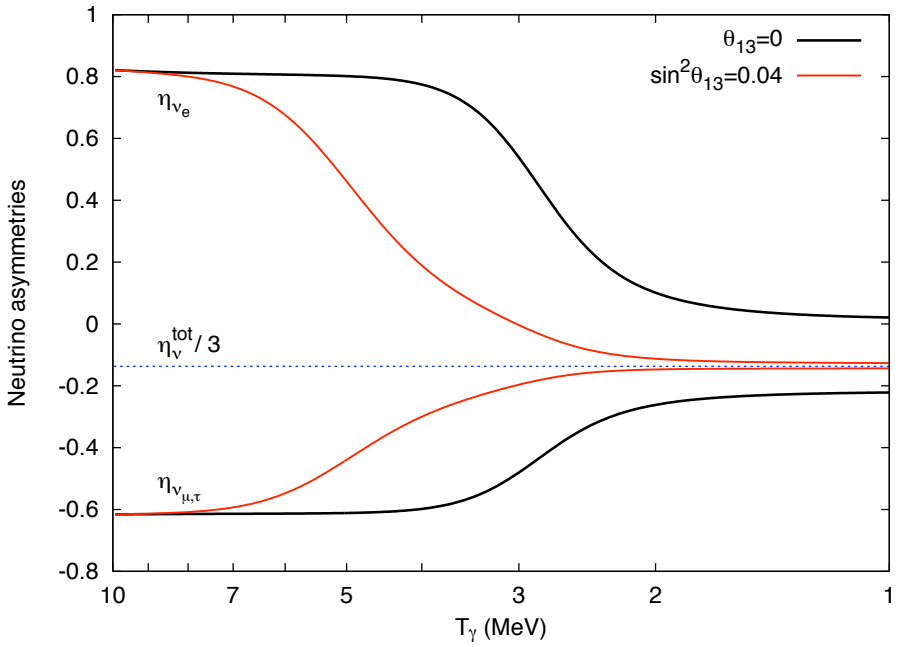

Figure 1. Evolution of the flavor neutrino asymmetries when $\eta_\nu = -0.41$, and $\eta^{\rm in}_{\nu_e} = 0.82$. The solid curves correspond to vanishing θ_{13} (outer black lines) and $\sin^2\theta_{13} = 0.04$ (inner red lines). The total neutrino asymmetry is constant and equal to three times the value shown (blue dotted line).

spectra in equilibrium. There is no full equipartition of the total η_ν among the three flavors, although collisions lead to final values of the flavor asymmetries closer to $\eta_\nu/3$ than those expected in an MSW matter neutrino conversion. In this case the final value of the electron neutrino asymmetry is close enough to zero at the onset of BBN to lie in the favored region. If $\sin^2\theta_{13} \lesssim 10^{-3}$, the outcome is very close to the case of vanishing θ_{13}.

In Figure 2 we show the final energy spectra of relic electron neutrinos and antineutrinos in arbitrary units for the same case of Figure 1 with vanishing θ_{13}. The upper (lower) solid line stands for the spectra of electron neutrinos (antineutrinos) calculated numerically, while the corresponding dotted lines are described by a Fermi/Dirac distribution just characterized by the same effective value of the electron neutrino degeneracy parameter (as used in all analyses before [21]). Both cases lead to the same value of the electron neutrino asymmetry but the real calculation shows that an excess of radiation in neutrinos remains.

In Figure 3 we show the evolution of the ratio of neutrino to photon energy densities, ρ_ν/ρ_γ, properly normalized so that it corresponds to $N_{\rm eff}$ at early and late times as in [21]. The fast drop of ρ_ν/ρ_γ at $T \sim 0.2$ MeV represents photon heating by e^+e^- annihilations. The case without asymmetries (dotted line) ends at late times at $N_{\rm eff} = 3.046$ instead of 3 because of residual neutrino heating [20]. We also show (solid lines) the evolution for our main example, where initially $N_{\rm eff} = 4.16$ for our choice of neutrino asymmetries. One can see that as soon as oscillations become effective reducing the flavor asymmetries, the excess of entropy is transferred from neutrinos to the electromagnetic plasma, cooling the former and heating the latter, but this process is only very effective for *large* values of θ_{13}. While the final $N_{\rm eff}$ is 3.1 for $\sin^2\theta_{13} = 0.04$, for negligible θ_{13} a significant deviation from equilibrium survives and leads to a final enhanced value of $N_{\rm eff} = 3.3$.

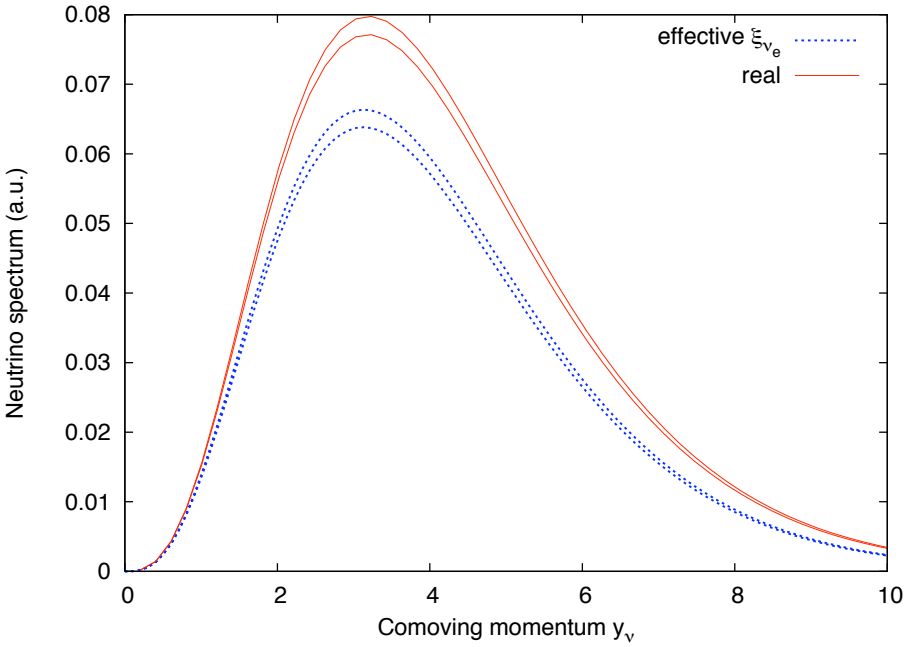

Figure 2. The final energy spectra of relic electron neutrinos and antineutrinos in arbitrary units for the same case of Figure 1 with vanishing θ_{13}. Upper (lower) solid line stands for electron neutrino (antineutrino) calculated numerically (label "real"). Upper (lower) dotted line stands for electron neutrino (antineutrino) described by a Fermi/Dirac distribution just characterized by the same effective value of the electron neutrino degeneracy parameter.

3 Results from BBN: constraints on total and electron neutrino asymmetries

As well known, BBN depends upon neutrino distribution functions in two ways. First of all, electron neutrinos and antineutrinos enter directly in the charge current weak processes which rule the neutron/proton chemical equilibrium. A change in the effective temperature of the distribution can shift the neutron/proton ratio freeze out temperature and thus modifies the primordial ^{4}He abundance. Similarly, a non-zero $\nu_e - \bar{\nu}_e$ asymmetry also changes chemical equilibrium towards a larger or smaller neutron fraction for negative or positive values of ξ_{ν_e}, respectively. Furthermore, lepton asymmetries in all flavors translate into a positive extra contribution to the neutrino energy density, speeding up the expansion rate given by the Hubble parameter.

Differently than in the approximated standard treatments, where both neutrino asymmetries and the extra contribution to $N_{\rm eff}$ due to ξ_{ν_α}, see eq. (1.3), are considered as constant parameters, in the present analysis we exactly follow the evolution of the neutrino distribution versus the photon temperature T_γ, which is our evolution parameter.[2] To this end we have changed the public numerical code `PArthENoPE` [22, 24] as follows. For any given initial values (at $T_\gamma = 10$ MeV) for the total neutrino asymmetry $\eta_\nu = \sum_\alpha \eta_{\nu_\alpha}$, unchanged by flavor oscillations, and electron neutrino asymmetry $\eta^{\rm in}_{\nu_e}$ we obtain, as described in the previous

[2]For another example of BBN calculations with arbitrarily-specified, time-dependent neutrino and antineutrino distribution functions, see Ref. [31].

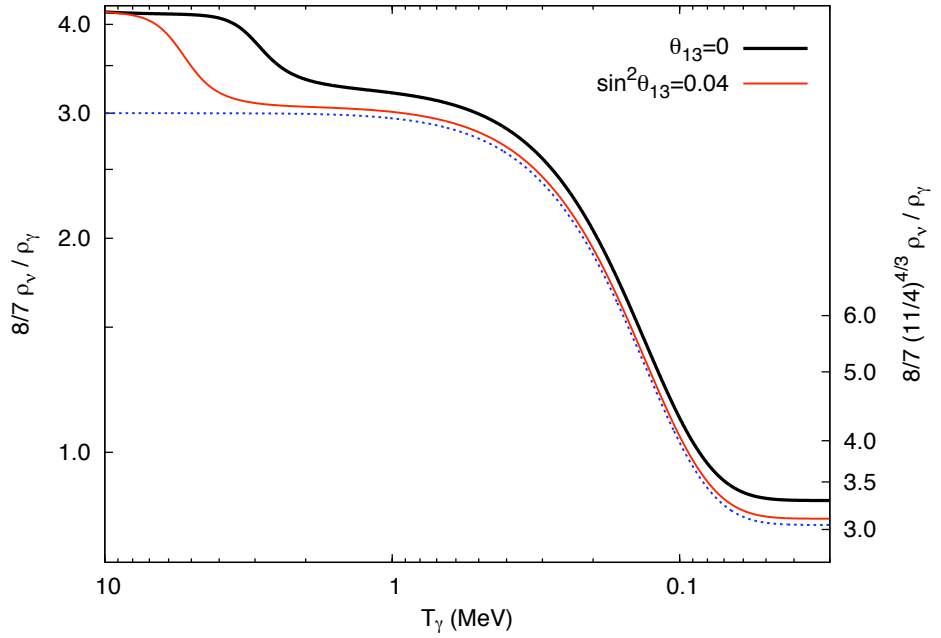

Figure 3. Evolution of the neutrino energy density for the same case as in Figure 1. The vertical axis is marked with $N_{\rm eff}$, left before e^+e^- annihilation, right afterwards. The solid curves correspond to vanishing θ_{13} (upper black line) and $\sin^2\theta_{13} = 0.04$ (lower red line). The case without asymmetries is shown for comparison (blue dotted line).

section, the time dependent neutrino distributions. The latter are then fitted in terms of Fermi-Dirac functions with the two evolving parameters $T_{\nu_\alpha}(T_\gamma)$ and $\xi_{\nu_\alpha}(T_\gamma)$. An example of their evolution is shown in Figure 4 for the same choice of initial asymmetries as in the case described in Section 2. Weak rates are then averaged over the corresponding electron (anti)neutrino distribution. The Hubble parameter is also modified to account for the actual evolution of total neutrino energy density.

The final abundances of both the ratio ^{2}H/H and the ^{4}He mass fraction, Y_p, are numerically computed as a function of the input parameters η_ν and $\eta^{\rm in}_{\nu_e}$ and compared with the corresponding experimental determinations. The baryon density parameter has been set to the value determined by the 7-year WMAP result, $\Omega_b h^2 = 0.02260 \pm 0.00053$ (68% C.L.) [5].[3]

To get confidence intervals for η_ν and $\eta^{\rm in}_{\nu_e}$, one can construct the likelihood function

$$\mathcal{L}(\eta_\nu, \eta^{\rm in}_{\nu_e}) \propto \exp\left(-\chi^2(\eta_\nu, \eta^{\rm in}_{\nu_e})/2\right) \quad , \tag{3.1}$$

with

$$\chi^2(\eta_\nu, \eta^{\rm in}_{\nu_e}) = \sum_{ij} [X_i(\eta_\nu, \eta^{\rm in}_{\nu_e}) - X_i^{obs}] W_{ij}(\eta_\nu, \eta^{\rm in}_{\nu_e}) [X_j(\eta_\nu, \eta^{\rm in}_{\nu_e}) - X_j^{obs}] \quad . \tag{3.2}$$

The proportionality constant can be obtained by requiring normalization to unity, and $W_{ij}(\eta_\nu, \eta^{\rm in}_{\nu_e})$ denotes the inverse covariance matrix [23],

$$W_{ij}(\eta_\nu, \eta^{\rm in}_{\nu_e}) = [\sigma^2_{ij} + \sigma^2_{i,exp}\delta_{ij} + \sigma^2_{ij,other}]^{-1} \quad , \tag{3.3}$$

[3]The allowed region of Ω_b in extended cosmological models with free $N_{\rm eff}$ does not differ significantly.

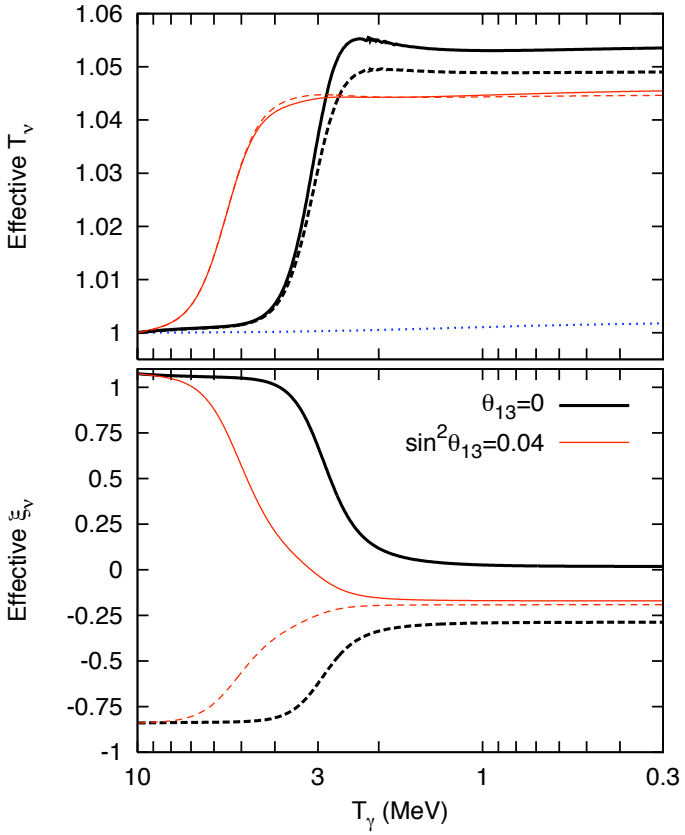

Figure 4. Evolution of the effective comoving temperatures and degeneracy parameters of electron (solid lines) and muon or tau (dashed lines) neutrinos for the same case as in Figure 1. Both the case of vanishing θ_{13} (thick black lines) and $\sin^2\theta_{13} = 0.04$ (thin red lines) are shown. The effective temperature for the case without asymmetries is shown in the upper panel for comparison (blue dotted line).

where σ_{ij} and $\sigma_{i,exp}$ represent the nuclear rate uncertainties and experimental uncertainties of nuclide abundance X_i, respectively [23], while by $\sigma^2_{ij,other}$ we denote the propagated squared error matrix due to all other input parameter uncertainties (τ_n, $G_{\rm N}$, $\Omega_b h^2$, ...). In our case we consider in eq. (3.2) as X_i the quantities ^{2}H/H and Y_p only.

Let us now briefly discuss the set of data we have used in our study. The ^{2}H/H number density is obtained by averaging seven determinations obtained in different Quasar Absorption Systems, as in [11]

$$^2{\rm H/H} = (2.87 \pm 0.22) \times 10^{-5} \ , \tag{3.4}$$

where the quadratic error has been enlarged by the value of the reduced χ^2 to account for the dispersion of measurements for this dataset, $\chi^2_{\rm min}/6 = 3.6$, see [11].

For the ^{4}He mass fraction we consider two different determinations. One is the result of the data collection analysis performed in [11],

$$Y_p = 0.250 \pm 0.003 \, . \tag{3.5}$$

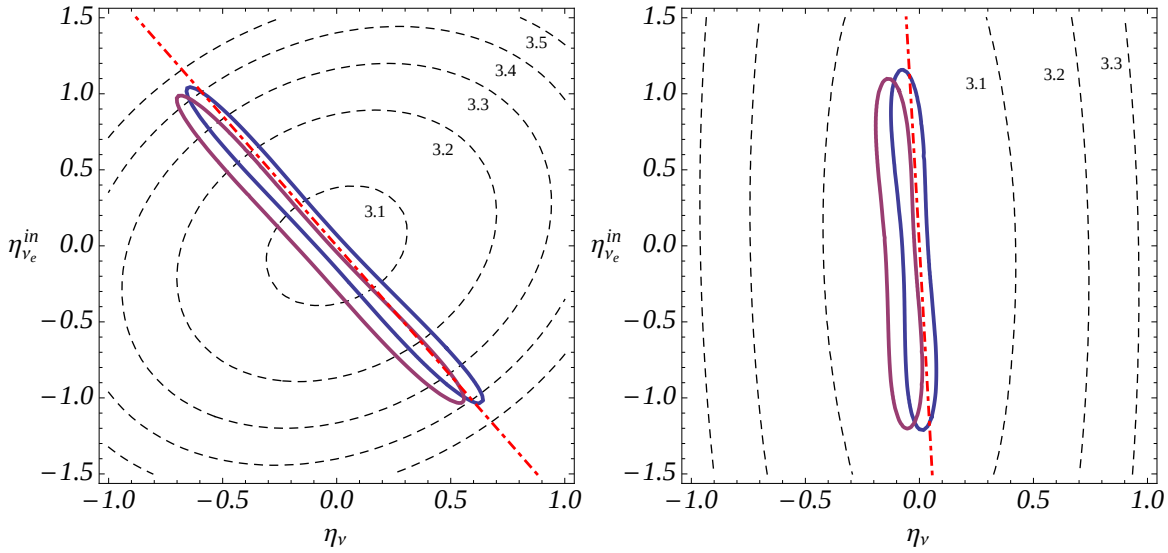

Figure 5. The 95% C.L. contours from our BBN analysis in the $\eta_\nu - \eta^{\rm in}_{\nu_e}$ plane for $\theta_{13} = 0$ (left) and $\sin^2\theta_{13} = 0.04$ (right). The two contours correspond to the different choices for the primordial ^{4}He abundances of eqs. (3.5) (blue) and (3.8) (purple). The (red) dot-dashed line is the set of values of η_ν and $\eta^{\rm in}_{\nu_e}$ which, due to flavor oscillations, evolve towards a vanishing final value of electron neutrino asymmetry $\eta^{\rm fin}_{\nu_e}$. We also report as dashed lines the iso-contours for different values of $N_{\rm eff}$, the effective number of neutrinos after e^+e^- annihilation stage.

More recently, new studies of metal poor H II regions have appeared in the literature [7–9]. While these groups both agree on a larger central value with respect to the result of eq. (3.5), which incidentally seems to pin down a value for $N_{\rm eff} > 3$ at 2σ, a different estimate of possible systematic effects which dominate the total uncertainty budget is quoted in [7] and [8], with [8] quoting a larger error, of the order of 4%.

$$Y_p = 0.2565 \pm 0.0010({\rm stat.}) \pm 0.0050({\rm syst.}) \quad [7] \ , \tag{3.6}$$

$$Y_p = 0.2561 \pm 0.0108 \quad [8] \ . \tag{3.7}$$

Finally, in a recent paper [9], Markov Chain Monte Carlo method was exploited to determine the ^{4}He abundance, and the uncertainties derived from observations of metal poor nebulae finding

$$Y_p = 0.2573 \pm 0.0033 \, . \tag{3.8}$$

In the following, we will use the two results of eq.s (3.5) and (3.8). While their uncertainties are the same, they differ for the central value, actually the smaller and higher of all results reported above, a fact which will produce two different bounds on the electron neutrino asymmetry.

The 95% C.L. contours for the total asymmetry η_ν and the initial value of the electron neutrino parameter $\eta^{\rm in}_{\nu_e}$ are shown in Figure 5 for the adopted determinations of ^{2}H and ^{4}He and for two different choices of θ_{13}. In both cases the contours are close to and aligned along the red dot-dashed line which represents the set of initial values for the asymmetries which eventually evolve toward a vanishing final electron neutrino asymmetry, $\eta^{\rm fin}_{\nu_e} \simeq 0$, which is preferred by ^{4}He data. We recall that ^{4}He is strongly changed if neutron/proton chemical

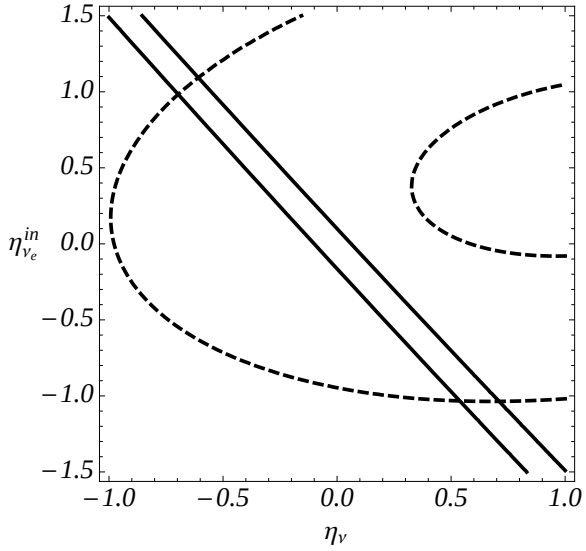

Figure 6. Bounds in the $\eta^{\rm in}_{\nu_e}$ - η_ν plane for each nuclear yield. Areas between the lines correspond to 95% C.L. regions singled out by the ^{4}He mass fraction (solid lines) of eq. (3.5), and Deuterium (dashed lines) as in eq. (3.4).

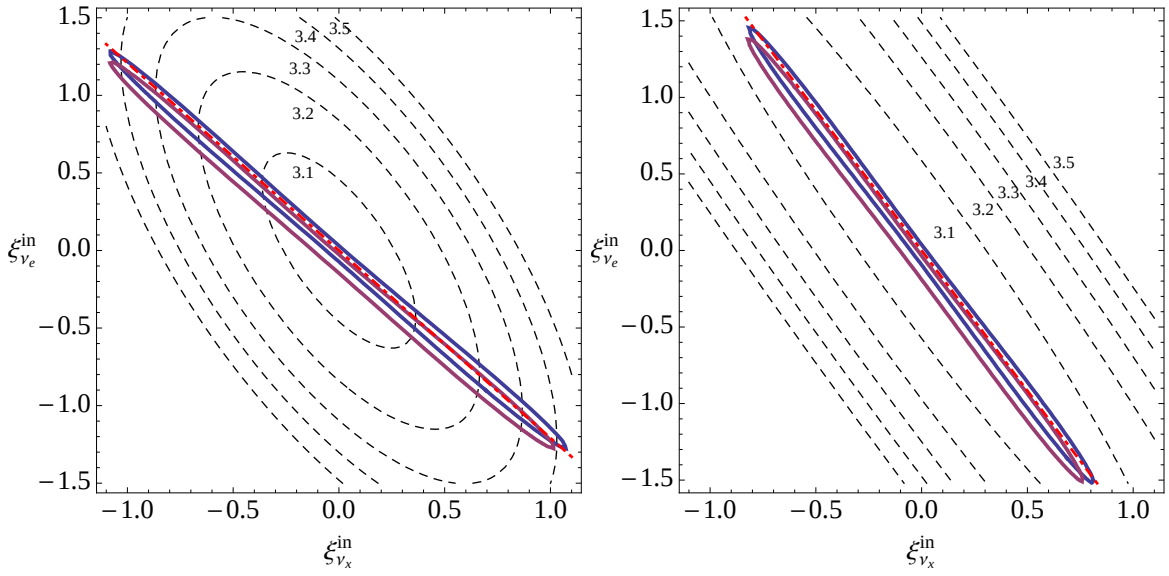

Figure 7. Same results as in Figure 5 in the plane of initial flavor degeneracy parameters $\xi^{\rm in}_{\nu_x}$ and $\xi^{\rm in}_{\nu_e}$.

equilibrium is shifted by a large value of $\nu_e - \bar{\nu}_e$ asymmetry around the freezing of weak rates ($T_\gamma \sim 0.8$ MeV). For large θ_{13}, oscillations efficiently mix all neutrino flavors and at BBN $\eta_{\nu_\alpha} \sim \eta_\nu/3$, so the bound on η_ν is quite stringent, $-0.1 \lesssim \eta_\nu \lesssim 0.1$, if we adopt the value of eq. (3.5) for Y_p. Instead, for the choice of eq. (3.8) we find $-0.20 \lesssim \eta_\nu \lesssim 0$, i.e. a larger value for Y_p singles out slightly negative values for η_ν (and $\eta^{\rm fin}_{\nu_e}$), since the theoretical prediction for Y_p grows in this case as the neutron-proton chemical equilibrium shift towards a larger

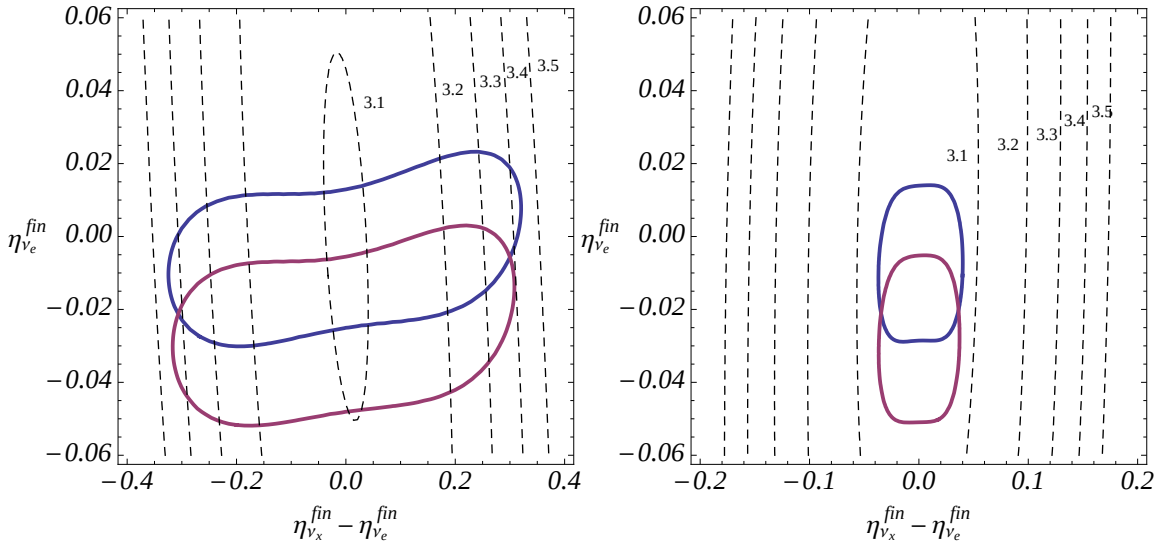

Figure 8. Same results as in Figure 5 in the plane of $\eta_{\nu_e}^{\rm fin}$ and the difference $\eta_{\nu_x}^{\rm fin} - \eta_{\nu_x}^{\rm fin}$, where the superscript indicates that the asymmetries are evaluated at the onset of BBN, $T_\gamma \sim 1$ MeV, after flavor oscillations shuffled the initial $\eta_{\nu_\alpha}^{\rm in}$.

	$\theta_{13} = 0$	$\sin^2\theta_{13} = 0.04$
$Y_p = 0.250 \pm 0.003$	$-0.66 < \eta_\nu < 0.63$	$-0.13 < \eta_\nu < 0.07$
$Y_p = 0.2573 \pm 0.0033$	$-0.71 < \eta_\nu < 0.56$	$-0.20 < \eta_\nu < 0.02$

Table 1. BBN bounds on the initial total neutrino asymmetry at 95% C.L.

neutron fraction at freeze-out . On the other hand, for a vanishing θ_{13} the contours for η_ν and $\eta_{\nu_e}^{\rm in}$ show a clear anticorrelation, and even values of order unity for both parameters are still compatible with BBN. The allowed regions of the total neutrino asymmetry are summarized in Table 1.

We stress that for any value of θ_{13}, the data on primordial deuterium, eq. (3.4), is crucial for closing the allowed region that the ^{4}He bound fixes along the $\eta_{\nu_e}^{\rm fin} \simeq 0$ line. In fact, though ^{2}H is less sensitive than ^{4}He to neutrino asymmetries and effective temperature which enter the Universe expansion rate, see e.g. [11], yet including it in the analysis breaks the degeneracy between $\eta_{\nu_e}^{\rm in}$ and η_ν which is present when only ^{4}He is used. This can be read from Figure 6 where the 95% C.L. in the $\eta_{\nu_e}^{\rm in}$ - η_ν plane are shown for ^{4}He and ^{2}H separately, for the case $\theta_{13} = 0$. The solid lines bound the region of the plane compatible with the ^{4}He measurement as in eq. (3.5), whereas the dashed contours correspond to Deuterium observation, see eq. (3.4). The different shape of these two regions is due to the different dependence of nuclide abundances on $\eta_{\nu_e}^{\rm in}$ and η_ν, thus their combination breaks the degeneracy and leads to a close contour as shown in Figure 5.

It is also interesting to report our results in terms of other variables, as in Figures 7 and 8. In the first case, the BBN contours are shown in the plane of initial flavor degeneracy parameters $\xi_{\nu_e}^{\rm in}$ and $\xi_{\nu_x}^{\rm in}$ while, in Figure 8, we consider a new pair of variables: the electron neutrino asymmetry at the onset of BBN $\eta_{\nu_e}^{\rm fin}$, and the difference $\eta_{\nu_x}^{\rm fin} - \eta_{\nu_e}^{\rm fin}$, which in the

standard analysis is usually assumed to be vanishing. One can see from this figure that, while the (95% C.L.) bound on $\eta^{\rm fin}_{\nu_e}$ is independent of the value of θ_{13}

$$-0.03 \leq \eta^{\rm fin}_{\nu_e} \leq 0.02\,, \quad \text{for } Y_p = 0.250 \pm 0.003 \ , \tag{3.9}$$

$$-0.05 \leq \eta^{\rm fin}_{\nu_e} \leq 0.003\,, \quad \text{for } Y_p = 0.2573 \pm 0.0033 \ , \tag{3.10}$$

the difference between the final ν_e and ν_x asymmetries strongly depends upon this yet unknown mixing angle, as expected. In fact, for large θ_{13} we recover the standard result, $\eta^{\rm fin}_{\nu_x} \sim \eta^{\rm fin}_{\nu_e}$, due to efficient mixing by oscillations and collisions, while for $\theta_{13} = 0$ the two asymmetries can be different. The following ranges are in good agreement with BBN data at 95 % C.L., *independently* of the adopted value for Y_p

$$-0.3 \leq \eta^{\rm fin}_{\nu_x} - \eta^{\rm fin}_{\nu_e} \leq 0.3\,, \quad \sin^2\theta_{13} = 0 \ , \tag{3.11}$$

$$-0.04 \leq \eta^{\rm fin}_{\nu_x} - \eta^{\rm fin}_{\nu_e} \leq 0.04\,, \quad \sin^2\theta_{13} = 0.04 \ . \tag{3.12}$$

We conclude that, in particular for $\theta_{13} = 0$ oscillations lead to quite different neutrino asymmetries in e and μ/τ flavors, still being in good agreement with BBN, differently than what was previously assumed in the literature, see [1–4], and [11–19] for BBN analyses.

In Figures 5-8 we also plot iso-contours for the value of the effective number of neutrinos, $N_{\rm eff}$, evaluated after e^+e^- annihilations. For large θ_{13} BBN data bound $N_{\rm eff}$ to be very close to the standard value 3.046, since all asymmetries should be very small in this case and flavor oscillations modify the neutrino distributions while neutrinos are still strongly coupled to the electromagnetic bath. Therefore, we do not expect non-thermal features in the neutrino spectra in this case, since scatterings and pair processes allow for an efficient transfer of any entropy excess. On the other hand, for vanishing θ_{13}, larger values of $N_{\rm eff}$ are still compatible with BBN data, up to values of the order of 3.4 at 95% C.L. The dependence of the largest achievable value of $N_{\rm eff}$ on the value of the mixing angle θ_{13}, obtained by spanning in the asymmetry parameter plane the region compatible with BBN, is reported in Figure 9.

It is worth noticing that the final values of $N_{\rm eff}$, in particular for large final asymmetries of ν_x, are also slightly larger than the $N_{\rm eff}$ that one would obtain using the equilibrium expression of eq. (1.2). For example, if we take $\eta^{\rm fin}_{\nu_e} = 0$ and $\eta^{\rm fin}_{\nu_x} = 0.3$, a point on the boundary of the BBN contours (see Figure 8) and compute the corresponding effective chemical potentials, using eq. (1.3) one gets $N_{\rm eff} = 3.2$, while the actual value is larger, $N_{\rm eff} = 3.4$, a signal that in this case the interplay of solar-like oscillations and neutrino freeze-out has produced indeed, a mild non-thermal distortion in neutrino distributions.

Finally, we notice that our BBN results correspond to a minimal scenario with primordial neutrino asymmetries, as we do not consider a possible extra contribution to $N_{\rm eff}$ coming from relativistic degrees of freedom other than standard active neutrinos. Their effect is known to produce looser bounds on neutrino asymmetries, as they speed up expansion and thus, can compensate the effect of a positive $\nu_e - \bar{\nu}_e$ asymmetry. We have explicitly checked that, for some choices of primordial asymmetries, the addition of extra radiation does not modify the evolution of flavor neutrino asymmetries. Of course, in such a case the contribution to the energy density of the additional relativistic degrees of freedom adds up to the surviving excess to $N_{\rm eff}$ arising from neutrino asymmetries.

4 Conclusions

In this paper we have calculated the evolution of neutrinos in the early universe with initial flavor asymmetries, taking into account the combined effect of collisions and oscillations. Our

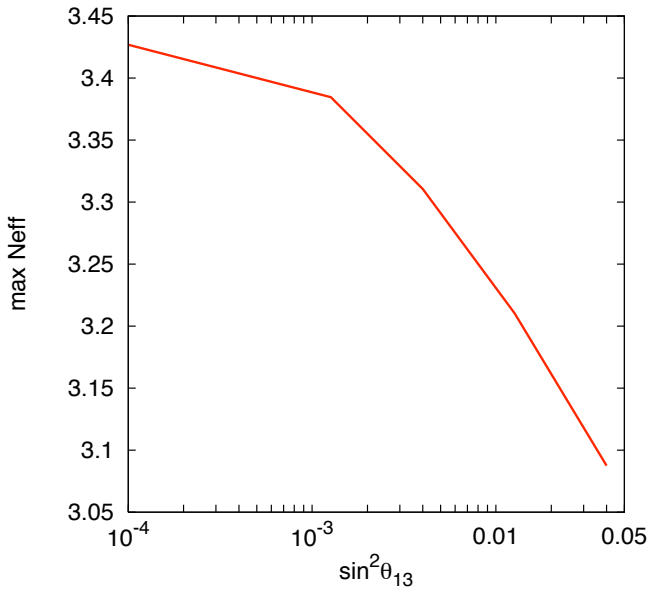

Figure 9. Largest values of $N_{\rm eff}$ from primordial neutrino asymmetries compatible with BBN, as a function of θ_{13}.

numerical results for the neutrino momentum distributions, which can develop non-thermal features, were used to find the primordial production of light elements, employing a modified version of the `PArthENoPE` BBN code. Comparing with the recent data on primordial ^{2}H and ^{4}He abundances, we have found the allowed ranges for both the total asymmetry and the initial asymmetry in electronic flavor. These BBN limits mostly depend on the value of θ_{13}, the only unknown mixing angle of neutrinos. As can be seen from Figure 9, for $\sin^2\theta_{13} \lesssim 10^{-3}$ this implies an effective number of neutrinos bound to $N_{\rm eff} \lesssim 3.4$, independently of which of the experimental ^{4}He mass fraction of eq.s (3.5) and (3.8) is adopted, whereas for larger values of θ_{13} the effective number of neutrinos is closely bound to the standard value 3.046 obtained for vanishing asymmetries.

In the near future it will be possible to improve our BBN constraints on the lepton number of the universe. On one hand, thanks to the better sensitivity of new neutrino experiments, either long-baseline or reactor, we expect to have a very stringent bound on θ_{13} or eventually its measurement (see e.g. [32]). Such results would lead to a more restrictive BBN analysis on primordial asymmetries. On the other hand, in the next couple of years data on the anisotropies of the cosmic microwave background from the Planck satellite [33] will largely reduce the allowed range of $N_{\rm eff}$, since the forecast sensitivity is of the order of 0.4 at 2σ [34–36]. Indeed, suppose that Planck data confirm a value of $N_{\rm eff} > 3$. An excess of radiation up to $0.4-0.5$ could imply the presence of a significative degeneracy in the neutrino sector, but this would depend on the result of θ_{13} measurement. A vanishing θ_{13} would allow such possibility, but a measured θ_{13} in the next generation of experiments *would imply* the presence of extra degrees of freedom others than active neutrinos. In case of a much larger

result by Planck, namely $N_{\rm eff} > 4$, it would be impossible to explain such a result in terms of primordial neutrino asymmetries only, and alternative cosmological scenarios with additional relativistic species, such as sterile neutrinos (see for instance [37]) would be strongly favored.

Acknowledgments

We would like to thank Georg Raffelt for his useful comments on an earlier version of this paper. G. Mangano, G. Miele, O. Pisanti and S. Sarikas acknowledge support by the *Istituto Nazionale di Fisica Nucleare* I.S. FA51 and the PRIN 2010 "Fisica Astroparticellare: Neutrini ed Universo Primordiale" of the Italian *Ministero dell'Istruzione, Università e Ricerca.* S. Pastor was supported by the Spanish grants FPA2008-00319 and Multidark CSD2009-00064 (MICINN) and PROMETEO/2009/091 (Generalitat Valenciana), and by the EC contract UNILHC PITN-GA-2009-237920. This research was also supported by a Spanish-Italian MICINN-INFN agreement, refs. FPA2008-03573-E and ACI2009-1051.

References

[1] C. Lunardini and A.Yu. Smirnov, *High-energy neutrino conversion and the lepton asymmetry in the universe*, *Phys. Rev. D* **64** (2001) 073006 [arXiv:hep-ph/0012056].

[2] A.D. Dolgov, S.H. Hansen, S. Pastor, S.T. Petcov, G.G. Raffelt and D.V. Semikoz, *Cosmological bounds on neutrino degeneracy improved by flavor oscillations*, *Nucl. Phys. B* **632** (2002) 363 [arXiv:hep-ph/0201287].

[3] Y.Y.Y. Wong, *Analytical treatment of neutrino asymmetry equilibration from flavour oscillations in the early universe*, *Phys. Rev. D* **66** (2002) 025015 [arXiv:hep-ph/0203180].

[4] K.N. Abazajian, J.F. Beacom and N.F. Bell, *Stringent constraints on cosmological neutrino antineutrino asymmetries from synchronized flavor transformation*, *Phys. Rev. D* **66** (2002) 013008 [arXiv:astro-ph/0203442].

[5] E. Komatsu et al., *Seven-Year Wilkinson Microwave Anisotropy Probe (WMAP) Observations: Cosmological Interpretation*, *Astrophys. J. Suppl. Ser.* **192** (2011) 18 [arXiv:1001.4538 [astro-ph.CO]].

[6] V.B. Semikoz, D.D. Sokoloff and J.W.F. Valle, *Is the baryon asymmetry of the Universe related to galactic magnetic fields?*, *Phys. Rev. D* **80** (2009) 083510 [arXiv:0905.3365 [hep-ph]].

[7] Y.I. Izotov and T.X. Thuan, *The primordial abundance of 4He: evidence for non-standard big bang nucleosynthesis*, *Astrophys. J.* **710** (2010) L67 [arXiv:1001.4440 [astro-ph.CO]].

[8] E. Aver, K.A. Olive and E.D. Skillman, *A New Approach to Systematic Uncertainties and Self-Consistency in Helium Abundance Determinations*, *JCAP* **1005** (2010) 003 [arXiv:1001.5218 [astro-ph.CO]].

[9] E. Aver, K.A. Olive and E.D. Skillman, *Mapping systematic errors in helium abundance determinations using Markov Chain Monte Carlo*, preprint arXiv:1012.2385 [astro-ph.CO].

[10] H.S. Kang and G. Steigman, *Cosmological Constraints on Neutrino Degeneracy*, *Nucl. Phys. B* **372** (1992) 494.

[11] F. Iocco, G. Mangano, G. Miele, O. Pisanti and P.D. Serpico, *Primordial Nucleosynthesis: from precision cosmology to fundamental physics*, *Phys. Rep.* **472** (2009) 1 [arXiv:0809.0631 [astro-ph]].

[12] S.H. Hansen, G. Mangano, A. Melchiorri, G. Miele and O. Pisanti, *Constraining neutrino physics with BBN and CMBR*, *Phys. Rev. D* **65** (2002) 023511 [arXiv:astro-ph/0105385].

[13] V. Barger, J.P. Kneller, H.S. Lee, D. Marfatia and G. Steigman, *Effective number of neutrinos and baryon asymmetry from BBN and WMAP*, *Phys. Lett. B* **566** (2003) 8 [arXiv:hep-ph/0305075].

[14] V. Barger, J.P. Kneller, P. Langacker, D. Marfatia and G. Steigman, *Hiding relativistic degrees of freedom in the early universe*, *Phys. Lett. B* **569** (2003) 123 [arXiv:hep-ph/0306061].

[15] A. Cuoco, F. Iocco, G. Mangano, G. Miele, O. Pisanti and P.D. Serpico, *Present status of primordial nucleosynthesis after WMAP: results from a new BBN code*, *Int. J. Mod. Phys. A* **19** (2004) 4431 [arXiv:astro-ph/0307213].

[16] R.H. Cyburt, B.D. Fields, K.A. Olive and E. Skillman, *New BBN limits on physics beyond the standard model from He-4*, *Astropart. Phys.* **23** (2005) 313 [arXiv:astro-ph/0408033].

[17] P.D. Serpico and G.G. Raffelt, *Lepton asymmetry and primordial nucleosynthesis in the era of precision cosmology*, *Phys. Rev. D* **71** (2005) 127301 [arXiv:astro-ph/0506162].

[18] V. Simha and G. Steigman, *Constraining The Universal Lepton Asymmetry*, *JCAP* **0808** (2008) 011 [arXiv:0806.0179 [hep-ph]].

[19] L.M. Krauss, C. Lunardini and C. Smith, *Neutrinos, WMAP, and BBN*, arXiv:1009.4666 [hep-ph].

[20] G. Mangano, G. Miele, S. Pastor, T. Pinto, O. Pisanti and P.D. Serpico, *Relic neutrino decoupling including flavour oscillations*, *Nucl. Phys. B* **729** (2005) 221 [arXiv:hep-ph/0506164].

[21] S. Pastor, T. Pinto and G.G. Raffelt, *Relic density of neutrinos with primordial asymmetries*, *Phys. Rev. Lett.* **102** (2009) 241302 [arXiv:0808.3137 [astro-ph]].

[22] O. Pisanti, A. Cirillo, S. Esposito, F. Iocco, G. Mangano, G. Miele and P.D. Serpico, *PArthENoPE: Public Algorithm Evaluating the Nucleosynthesis of Primordial Elements*, *Comput. Phys. Commun.* **178** (2008) 956 [arXiv:0705.0290 [astro-ph]].

[23] P.D. Serpico, S. Esposito, F. Iocco, G. Mangano, G. Miele and O. Pisanti, *Nuclear Reaction Network for Primordial Nucleosynthesis: a detailed analysis of rates, uncertainties and light nuclei yields*, *JCAP* **0412** (2004) 010 [arXiv:astro-ph/0408076].

[24] `PArthENoPE` web page: http://parthenope.na.infn.it/

[25] J. Gava and C. Volpe, *CP violation effects on the neutrino degeneracy parameters in the Early Universe*, *Nucl. Phys. B* **837** (2010) 50 [arXiv:1002.0981 [hep-ph]].

[26] G. Sigl and G. Raffelt, *General kinetic description of relativistic mixed neutrinos*, *Nucl. Phys. B* **406** (1993) 423.

[27] B.H. McKellar and M.J. Thomson, *Oscillating doublet neutrinos in the early universe*, *Phys. Rev. D* **49** (1994) 2710.

[28] T. Schwetz, M.A. Tórtola and J.W.F. Valle, *Three-flavour neutrino oscillation update*, *New J. Phys.* **10** (2008) 113011 [arXiv:0808.2016 [hep-ph]].

[29] G.L. Fogli, E. Lisi, A. Marrone, A. Palazzo and A.M. Rotunno, *Hints of $\theta_{13} > 0$ from global neutrino data analysis*, *Phys. Rev. Lett.* **101** (2008) 141801 [arXiv:0806.2649 [hep-ph]].

[30] M.C. González-García, M. Maltoni and J. Salvado, *Updated global fit to three neutrino mixing: status of the hints of $\theta_{13} > 0$*, *JHEP* **1004** (2010) 056 [arXiv:1001.4524 [hep-ph]].

[31] C.J. Smith, G.M. Fuller and M.S. Smith, *Big Bang Nucleosynthesis with Independent Neutrino Distribution Functions*, *Phys. Rev. D* **79** (2009) 105001 [arXiv:0812.1253 [astro-ph]].

[32] P. Huber, M. Lindner, M. Rolinec, T. Schwetz and W. Winter, *Prospects of accelerator and reactor neutrino oscillation experiments for the coming ten years*, *Phys. Rev. D* **70** (2004) 073014 [arXiv:hep-ph/0403068].

[33] Planck Collaboration, *Planck: The scientific programme*, preprint arXiv:astro-ph/0604069.

[34] R. Bowen, S.H. Hansen, A. Melchiorri, J. Silk and R. Trotta, *The Impact of an Extra Background of Relativistic Particles on the Cosmological Parameters derived from Microwave Background Anisotropies*, *Mon. Not. Roy. Astron. Soc.* **334** (2002) 760 [arXiv:astro-ph/0110636].

[35] S. Bashinsky and U. Seljak, *Signatures of relativistic neutrinos in CMB anisotropy and matter clustering*, *Phys. Rev. D* **69** (2004) 083002 [arXiv:astro-ph/0310198].

[36] J. Hamann, S. Hannestad, J. Lesgourgues, C. Rampf and Y.Y.Y. Wong, *Cosmological parameters from large scale structure - geometric versus shape information*, *JCAP* **1007** (2010) 022 [arXiv:1003.3999 [astro-ph.CO]].

[37] A. Melchiorri, O. Mena, S. Palomares-Ruiz, S. Pascoli, A. Slosar and M. Sorel, *Sterile Neutrinos in Light of Recent Cosmological and Oscillation Data: a Multi-Flavor Scheme Approach*, *JCAP* **0901** (2009) 036 [arXiv:0810.5133 [hep-ph]].